

Climate variability in the SE Alps of Italy over the past 17 000 years reconstructed from a stalagmite record

SILVIA FRISIA, ANDREA BORSATO, CHRISTOPH SPÖTL, IGOR M. VILLA AND FRANCO CUCCHI

BOREAS



Frisia, S., Borsato, A., Spötl, C., Villa, I. M. & Cucchi, F. 2005 (November): Climate variability in the SE Alps of Italy over the past 17 000 years reconstructed from a stalagmite record. *Boreas*, Vol. 34, pp. 445–455. Oslo. ISSN 0300-9483.

Stalagmite SV1 from Grotta Savi, located at the SE margin of the European Alps (Italy), is the first Alpine speleothem that continuously spans the past *c.* 17 kyr. Extension rate and $\delta^{18}\text{O}_c$ record for the Lateglacial probably reflect a combination of temperature and rainfall, with rainfall exerting the dominant effect. Low speleothem calcite $\delta^{18}\text{O}_c$ values were recorded from *c.* 14.5 and 12.35 kyr, during GI-1 (Bølling–Allerød) interstadial, which, in our interpretation, was warm and wet. The GS-1 (Younger Dryas) was characterized by a shift to heavier $\delta^{18}\text{O}_c$, coinciding with $\delta^{13}\text{C}_c$ enrichment and extremely low extension rate ($<8 \mu\text{m}/\text{year}$). These characteristics indicate that GS-1 climate was cool and dry in the SE Alps. Calibration using historical data revealed that there is a positive $\delta^{18}\text{O}_c/dT$ relationship. A 1°C rise in mean annual temperature should correspond to *c.* 2.85‰ increase of SV-1 $\delta^{18}\text{O}_c$. We reconstructed a slow and steady temperature rise of *c.* 0.5°C since 10 kyr BP, in broad agreement with reconstructions from pollen data for SE Europe. Stalagmite SV1 indicates that climate variability in the SE Alps has been influenced by the Mediterranean Sea for the past *c.* 17 kyr.

Silvia Frisia (e-mail: frisia@mtsn.tn.it) and Andrea Borsato (e-mail: borsato@mtsn.tn.it), Museo Tridentino di Scienze Naturali, via Calepina 14, I-38100 Trento, Italy; Christoph Spötl (e-mail: Christoph.Spoetl@uibk.ac.at), Institut für Geologie und Paläontologie, Leopold-Franzens-Universität, Innrain 52, A-6020 Innsbruck, Austria; Igor M. Villa (e-mail: igor@geo.unibe.ch), Dipartimento di Scienze Geologiche e Geotecnologie, Università di Milano-Bicocca, I-20126 Milan, Italy, and Institut für Geologie, Isotopengeologie, Universität Bern, Erlachstrasse 9A, CH-3012 Berne, Switzerland; Franco Cucchi (e-mail: cucchi@univ.trieste.it), Dipartimento di Scienze Geologiche, Ambientali e Marine, Università di Trieste, Via Weiss, 2, I-34127 Trieste, Italy; received 20th October 2004, accepted 21st April 2005.

The European Alps is a region very sensitive to climatic change (Beniston & Jungo 2002), and it is important to extend the existing climate records as far back in time as possible to detect any anthropogenic climate signals. At present, there is a large set of palaeoclimate and climate data from the Central and Western Alps, but a fragmentary record from the Eastern Alps (cf. Davis *et al.* 2003 and references therein). A stalagmite record from northern Italy (McDermott *et al.* 1999) suggested that the Central Alps had a similar Holocene climatic evolution as the Jura Mountains and the French Alps. The eastern sector of the Italian Alps lies at the boundary between the Central and Southern European climate regions as defined by pollen data (Davis *et al.* 2003) and, therefore, may show different climate evolution with respect to the Central and Western Alps. The Eastern Italian Alps have great pre-history importance, which is documented by abundant archaeological evidence for both indigenous and imported cultural ‘packages’ (Mithen 2003). In the Dalmeri Shelter site, at 1240 m a.s.l. in NE Italy, a unique finding of painted stones dated at *c.* 13 cal. kyr BP, which show Iberian naturalistic influence (Dalmeri *et al.* 2004), seems to support Mithen’s (2003) hypothesis that the Younger

Dryas (YD) marked the end of the Palaeolithic painters. A better insight into the climate evolution of the SE European Alps from the Last Glacial Maximum would greatly improve our understanding of Alpine history. Here we present an exceptional *c.* 17 kyr speleothem record from the southeastern margin of the Italian Alps.

Sampling and analytical procedures

Geographical setting

The 27-cm-high, candle-shaped, stalagmite SV1 was sampled in Grotta Savi, a cave located at 441 m a.s.l. north of Trieste ($45^\circ37'05''\text{N}$, $13^\circ53'10''\text{E}$) (Fig. 1). The outer surface of the stalagmite was whitish, translucent and wet, a typical feature of active stalagmites from the southern watershed of the Alps. At the time of removal, SV1 was fed by a constant drip (*c.* 10 drops/min) from a stalactite growing about 30 m above the stalagmite. The Savi cave is cut in fissured limestone overlain by thin ($<50 \text{ cm}$) grassland soil cover, a situation which optimizes the potential for a rapid response to climate changes. The present-day

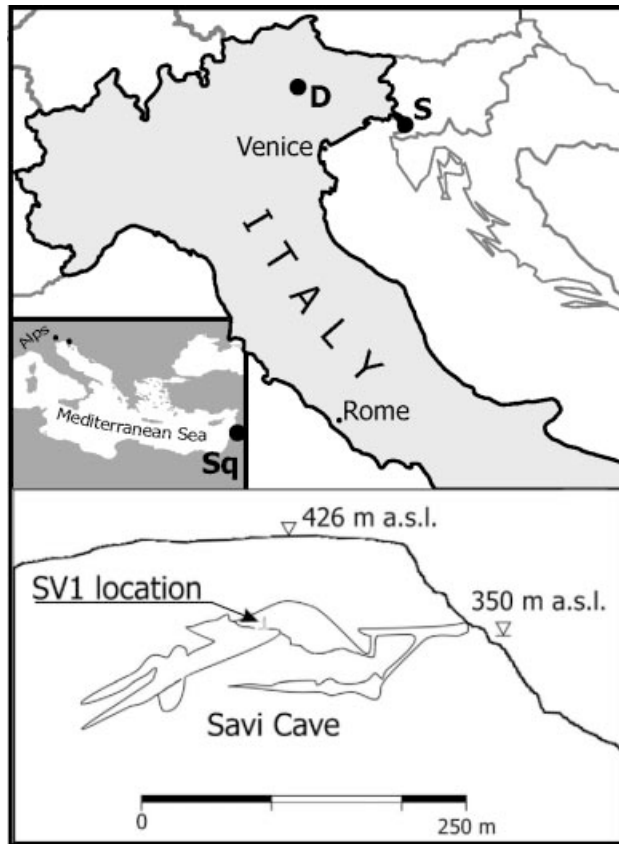


Fig. 1. Location of Savi Cave (S), geological setting and original position of stalagmite SV1 within Caverna Morpurgo passage. The map shows the location of the Late Palaeolithic Dalmeri Shelter (D) and Soreq Cave (Sq).

climate is sub-continental Mediterranean, characterized by long cool and dry winters, warm and dry summers and wet autumns. Mean winter and summer temperatures are $+1.5^{\circ}\text{C}$ and $+17.5^{\circ}\text{C}$, respectively. Below zero temperatures are recorded for about 70 days/year. The mean annual precipitation in Trieste is 1044 mm/year (years 1841 to 1996) with highest values in September (110 mm), October (126 mm) and November (105 mm). The inner part of the cave has a constant air and water temperature of $12.3 \pm 0.2^{\circ}\text{C}$.

Dating and age model

SV1 was cut parallel to its vertical growth axis, and its central portion (265 mm high) was examined in polished slabs and thin sections lying on an impure (clastic) base. The time scale of SV1 is based on a total of 18 U/Th ages measured with multiple-collector inductively coupled plasma mass spectrometry (MC-ICPMS) at the Laboratory of Isotope Geochemistry, University of Berne, Switzerland, on 150 to 250 mg calcite subsamples drilled in the axial part of the specimen (Fig. 2). Subsamples for U/Th dating were

dissolved and equilibrated with a mixed $^{236}\text{U} - ^{229}\text{Th}$ spike. Th and U were separated in columns containing an ion exchange resin. The ages were calculated by using the decay constants reported in Cheng *et al.* (2000) (Table 1). All samples had low U content (from 146 to 220 ppb) and the $^{230}\text{Th}/^{232}\text{Th}$ activity ratios were low (7 to 103), suggesting detrital contamination. Ages were therefore corrected for initial detrital Th by utilizing a $^{230}\text{Th}/^{232}\text{Th}$ activity ratio of the detrital component of $1.34^{+0.31}_{-0.25}$ (2σ error) (see Fig. 3 and Appendix), which yields corrections ranging from 1.3% (SV1 -24, -27, -28) up to 17% for subsamples with the highest detrital Th fraction (SV1-B1 e SV1-22) (Table 1). The age model is based on a linear interpolation between the corrected ages expressed in years (yr) or thousands of years (kyr) before the year 2000 (Fig. 3).

Stable isotopes

Samples for high-resolution stable isotope analysis were micromilled along the central axis of the top 37 mm of the stalagmite using a 0.3-mm fixed interval. In the lower part (37 to 265 mm), isotope samples were drilled at 1-mm intervals by using a 0.2-mm drill bit. In addition, we sampled individual growth layers from the axis laterally at five different levels (Fig. 2). The stable C and O isotope compositions were measured using a Delta^{plus} XL mass spectrometer equipped with an on-line automated carbonate preparation system (Gasbench II). Standardization was accomplished by using NBS19 standard, and the results are reported relative to the Vienna Pedee Belemnite (VPDB) standard. The 1σ precision of the $\delta^{18}\text{O}$ and $\delta^{13}\text{C}$ values is less than 0.1‰.

Results

SV1 started to form at 16.6 ± 0.5 kyr BP and grew almost continuously up to the present. It is the first European speleothem that preserves a continuous record for the past *c.* 17 kyr (Niggemann *et al.* (2003) provided a record from composite samples). The extension rate was very slow ($\leq 10 \mu\text{m}/\text{yr}$) up to 10.6 ± 0.22 kyr BP. From *c.* 10.6 to *c.* 7.5 kyr BP, SV1 records its highest extension rate (32 to 43 $\mu\text{m}/\text{yr}$). From *c.* 5.7 to *c.* 4.4 kyr BP there was another period of relatively fast growth (24 to 28 $\mu\text{m}/\text{yr}$), and then growth rate stabilized at 11 $\mu\text{m}/\text{yr}$ (Fig. 3).

SV1 is composed of elongated columnar calcite (Frisia *et al.* 2000) with visible growth laminae 1 to 50 μm thick (Fig. 4). Each lamina consists of a thicker, translucent calcite sublayer, and a 0.5 to 4 μm thin, brown, luminescent portion. The growth rate is relatively low, and some laminae are too thin to be resolved by optical microscopy, which hinders the possibility of precise lamina counting. These groups of

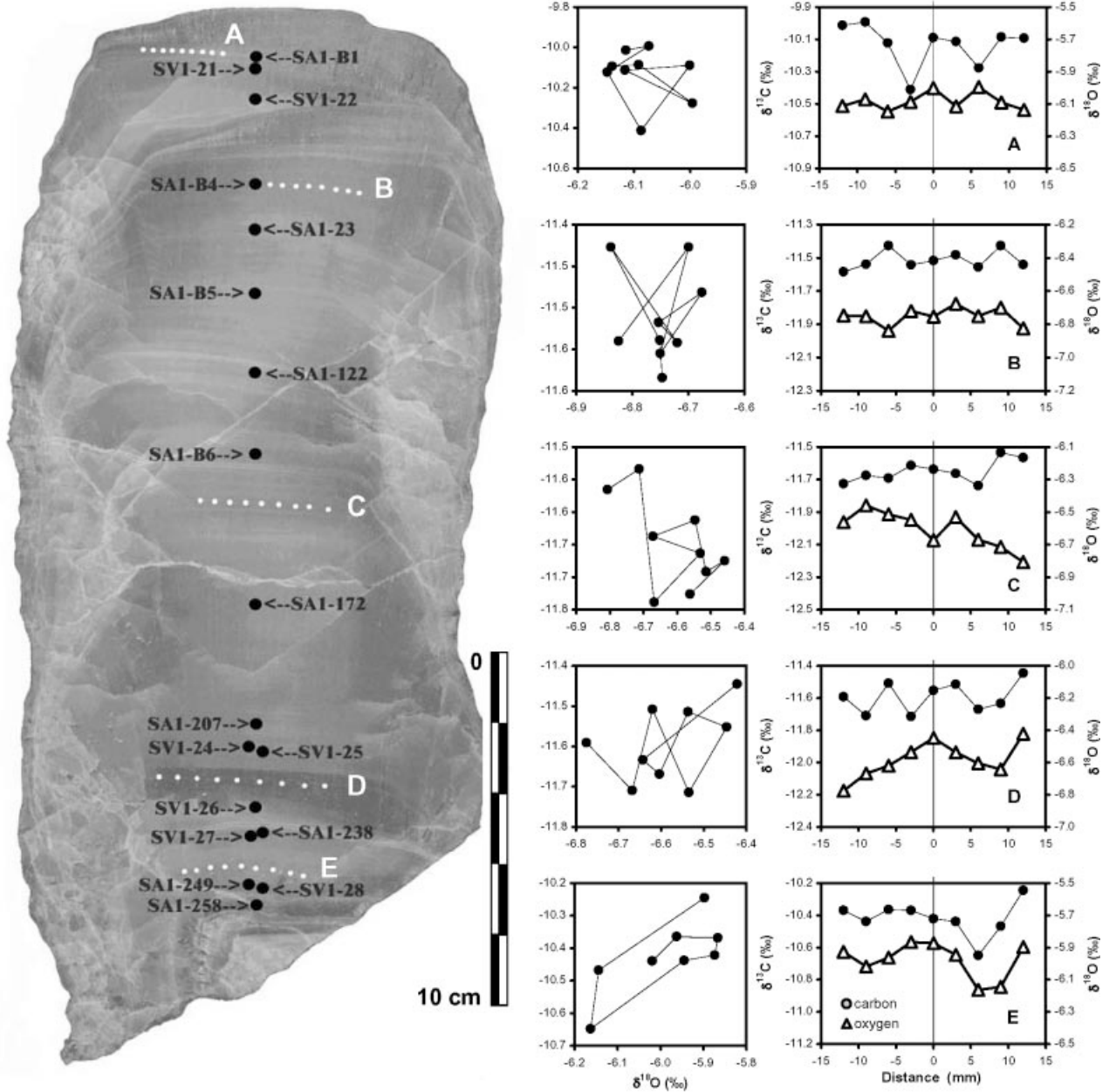


Fig. 2. Polished slab of stalagmite SV1 with the location of the U/Th samples (black dots). The small white dots indicate boreholes for the 'Hendy tests' (Hendy 1971) for isotopic equilibrium carried out at 12 (A), 50 (B), 144 (C), 220 (D) and 244 mm (E) from the stalagmite top, given on the diagrams to the right.

extremely thin laminae commonly appear as darker bands in thin section (Fig. 4). When the mean thickness of each lamina is consistent with the theoretical mean annual extension rate between two dated intervals, lamination is likely to be annual (from *c.* 10.6 to *c.* 7.5 kyr, and in the past 4 kyr). The elongated columnar calcite fabric that forms SV1 indicates that deposition occurred in quasi-equilibrium conditions

(Frisia *et al.* 2000). The five tests for isotopic equilibrium (Hendy 1971) show negligible kinetic effects (Fig. 2) with the exception of the bottom layer E, where $\delta^{13}\text{C}_c$ and $\delta^{18}\text{O}_c$ co-vary (a 0.4‰ increase in $\delta^{13}\text{C}_c$ is accompanied by a 0.2‰ in $\delta^{18}\text{O}_c$).

The resolution of the C and O isotope profiles varies according to sampling and extension rates. Between *c.* 16.6 and 10.6 kyr BP, mean resolution is 123 years,

Table 1. Results of U/Th analyses (errors are quoted as 2σ standard deviations). Ages were corrected for detrital thorium by utilizing the $^{230}\text{Th}/^{232}\text{Th}$ value of $1.34^{+0.31}/_{-0.25}$ (2σ errors).

Sample	Dist. mm	U	$^{234}\text{U}/^{238}\text{U}$	$^{230}\text{Th}/^{238}\text{U}$	$^{230}\text{Th}/^{232}\text{Th}$	$^{234}\text{U}/^{238}\text{U}$ (t=0)	Age	Age corr
		ppb	Activity ratio				kyr	kyr
SV1-B1	14.5	172.5 ± 0.49	0.9735 ± 0.0034	0.0139 ± 0.0011	7.5 ± 0.57	0.9735 ± 0.003	1.57 ± 0.13	1.29 + 0.17–0.19
SV1-21	18.5	178.9 ± 0.46	0.9729 ± 0.0034	0.0178 ± 0.0009	13.1 ± 0.64	0.9728 ± 0.003	2.02 ± 0.10	1.81 + 0.14–0.14
SV1-22	27.5	195.9 ± 0.56	0.9690 ± 0.0039	0.0258 ± 0.0008	7.6 ± 0.25	0.9688 ± 0.004	2.95 ± 0.10	2.43 + 0.21–0.24
SV1-B4	52.5	176.5 ± 0.46	0.9732 ± 0.0030	0.0406 ± 0.0015	27.4 ± 1.02	0.9729 ± 0.003	4.65 ± 0.17	4.43 + 0.21–0.24
SV1-23	62.3	163.3 ± 0.41	0.9745 ± 0.0028	0.0431 ± 0.0011	39.2 ± 1.03	0.9742 ± 0.003	4.94 ± 0.13	4.78 + 0.16–0.17
SV1-B5	83.8	220.8 ± 0.56	0.9870 ± 0.0018	0.0523 ± 0.0012	28.2 ± 0.65	0.9868 ± 0.002	5.95 ± 0.13	5.66 + 0.21–0.19
SV1 122	103.0	192.4 ± 0.54	0.9856 ± 0.0055	0.0704 ± 0.0014	18.1 ± 0.38	0.9853 ± 0.006	8.10 ± 0.17	7.52 + 0.30–0.33
SV1-B6r	127.0	168.5 ± 0.84	1.0103 ± 0.0110	0.0771 ± 0.0020	29.6 ± 1.62	1.0110 ± 0.011	8.67 ± 0.26	8.28 + 0.33–0.33
SV1-172	172.0	154.9 ± 0.48	1.0002 ± 0.0070	0.0859 ± 0.0016	25.9 ± 0.51	1.0002 ± 0.007	9.80 ± 0.19	9.32 + 0.29–0.32
SV1-207	207.0	168.6 ± 0.49	1.0020 ± 0.0053	0.0959 ± 0.0014	30.9 ± 0.50	1.0021 ± 0.006	10.98 ± 0.18	10.53 + 0.27–0.30
SV1-24	214.0	160.4 ± 0.42	0.9835 ± 0.0042	0.0926 ± 0.0018	69.7 ± 1.51	0.9829 ± 0.004	10.80 ± 0.23	10.66 + 0.25–0.25
SV1-25	215.0	175.9 ± 0.46	0.9883 ± 0.0044	0.0940 ± 0.0017	50.0 ± 1.08	0.9879 ± 0.005	10.92 ± 0.21	10.64 + 0.26–0.28
SV1-26	230.0	151.1 ± 0.40	0.9895 ± 0.0039	0.1196 ± 0.0020	27.0 ± 0.58	0.9890 ± 0.004	14.07 ± 0.26	13.41 + 0.40–0.43
SV1-238	238.0	179.5 ± 0.47	1.0039 ± 0.0032	0.1282 ± 0.0015	53.9 ± 0.71	1.0040 ± 0.003	14.92 ± 0.19	14.57 + 0.26–0.28
SV1-27	239.2	193.2 ± 0.50	0.9971 ± 0.0036	0.1266 ± 0.0017	86.3 ± 1.32	0.9969 ± 0.004	14.83 ± 0.22	14.62 + 0.25–0.27
SV1-249	249.0	159.6 ± 0.40	1.0130 ± 0.0036	0.1469 ± 0.0020	11.6 ± 0.17	1.0136 ± 0.004	17.11 ± 0.26	15.26 + 0.69–0.85
SV1-28	250.0	188.1 ± 0.48	1.0076 ± 0.0027	0.1331 ± 0.0015	103.3 ± 2.24	1.0080 ± 0.003	15.47 ± 0.20	15.33 + 0.22–0.22
SV1-258	257.5	146.3 ± 0.40	1.0184 ± 0.0041	0.1589 ± 0.0028	11.8 ± 0.22	1.0194 ± 0.004	18.51 ± 0.37	16.57 + 0.79–0.96

from *c.* 10.6 to 2.5 kyr BP it is 23 to 95 years (mean resolution = 28 years), and from 2.5 kyr BP to the present it is 18 to 25 years. The $\delta^{18}\text{O}_c$ values show a tendency toward lower values during the Lateglacial, from 16.6 to 10.6 kyr BP (-4.45‰ at 16.6 kyr to -6.65‰ at 10.6 kyr). The Lateglacial is characterized by $\delta^{18}\text{O}_c$ minima at *c.* 15.4, 14.5 and 12.3 kyr BP

(Fig. 5). In the Lateglacial, the interval from *c.* 12.0 to *c.* 11.4 kyr BP is marked by higher $\delta^{18}\text{O}_c$ values, and there is a drop of about 1‰ from *c.* 11.4 kyr to *c.* 10.6 kyr BP (Fig. 5). During the Holocene the $\delta^{18}\text{O}_c$ trend is a slow, steady rise of values. $\delta^{18}\text{O}_c$ minima are recorded from *c.* 6.4 to 6.0 kyr BP, at *c.* 4.5 kyr BP, from *c.* 3.0 to 2.5 kyr BP and from 0.2 to 0.6 kyr BP.

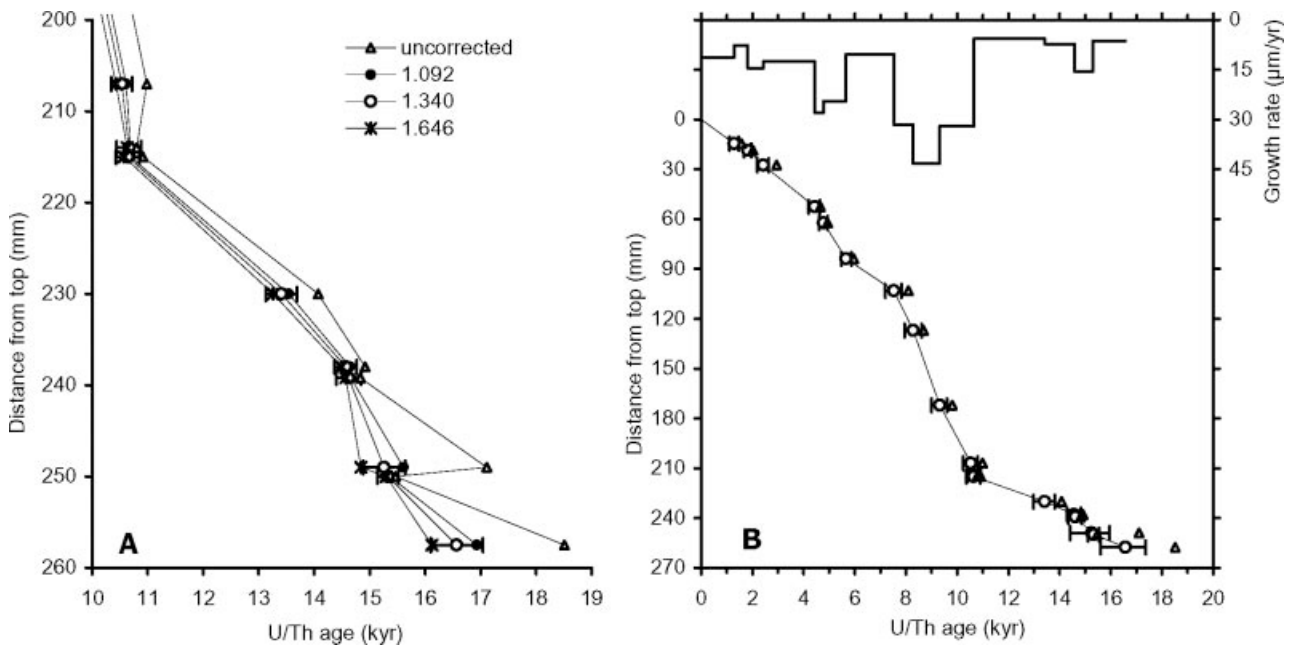


Fig. 3. A. Age model for SV1. Triangles = uncorrected ages; dots, open circles and asterisks indicate the corrected ages calculated with a $^{230}\text{Th}/^{232}\text{Th}$ activity ratio for the detrital component of 1.092, 1.340 and 1.646, respectively. The 2σ error bars are plotted only for the 1.340 corrected series. B. Age model and mean annual extension rate for SV1. Triangles = uncorrected ages; open circles = ages corrected for $^{230}\text{Th}/^{232}\text{Th}$ activity ratio of the detrital component of $1.34^{+0.31}/_{-0.25}$. The corrected ages are plotted with 2σ error bars.

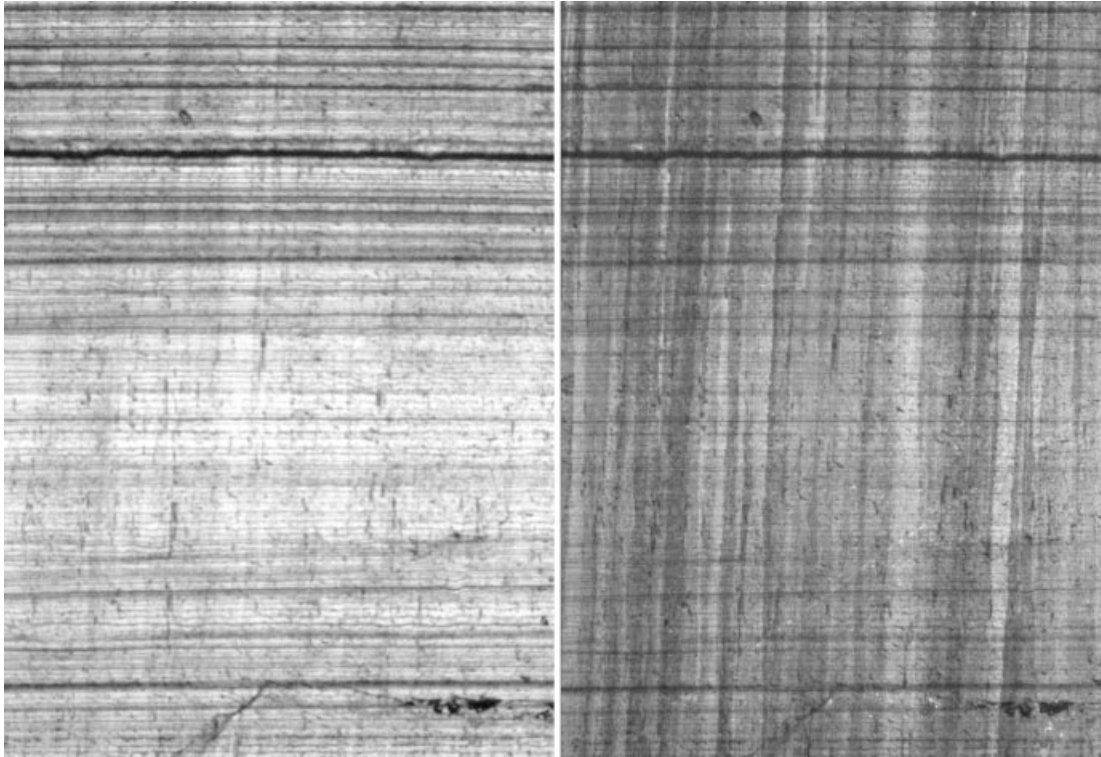


Fig. 4. Micrograph showing the laminated columnar calcite fabric typical of SV1. Left: transmitted light; right: cross-polarized light. Height of the micrograph = 7 mm.

The past 200 years are characterized by relatively high $\delta^{18}\text{O}_c$ values. The C isotope profile shows a trend toward more depleted values (from -8.9‰ to -11.3‰) in the Lateglacial, with the exception of the 12.0 to c. 11.4 kyr BP interval, where $\delta^{13}\text{C}_c$ and $\delta^{18}\text{O}_c$ co-vary (Fig. 5). This time period corresponds to a honey-coloured layer in the columnar fabric (Fig. 2). The Holocene C isotope trend is relatively stable, from -11.3‰ to -11.9‰ between 10.6 and 1.7 kyr BP. In the last 1.7 kyr the trend is reversed to higher $\delta^{13}\text{C}_c$ values (from -11.9‰ to -10.8‰).

Discussion

Calibration of the oxygen isotope values for the Holocene

It is common in palaeoclimate reconstruction to assume that the present is the key to the past (Bar-Matthews *et al.* 2003; Darling 2004). We apply this same assumption to the Holocene part of the record. The top of SV1 has a $\delta^{18}\text{O}_c$ value of -6.1‰ . The equilibrium calcite-water isotopic fractionation factor at the cave temperature of 12.3°C is $+1.1\text{‰}$ (Craig 1961; O'Neil *et al.* 1969). The theoretical $\delta^{18}\text{O}$ value of the formation water would range from $\delta^{18}\text{O}_w = -7.2\text{‰}$ to $\delta^{18}\text{O}_w = -6.7\text{‰}$ (VSMOW) according to the equation used for the calculation. The mean

monthly $\delta^{18}\text{O}_w$ value measured for 7 drip-water specimens collected from March to September 2003 in Caverna Morpurgo is $-7.28 \pm 0.22\text{‰}$ (VSMOW). The mean $\delta^{18}\text{O}_w$ value for the drip-waters is similar to the mean annual $\delta^{18}\text{O}_p$ of the precipitation waters (-7.36‰ VSMOW) measured at the nearby Basovizza weather station (Longinelli & Selmo 2003). Kinetic effects affecting the infiltration water are therefore negligible and the $\delta^{18}\text{O}_w$ reflects the $\delta^{18}\text{O}_p$.

Stalagmite oxygen isotopic records can be calibrated using historical data (Lauritzen & Lundberg 1999). The top 5.5 mm of the stalagmite should correspond to the past 500 years, at the estimated growth rate of $11\ \mu\text{m}/\text{yr}$. A reconstruction of temperature anomalies in the Alps is available for the past 500 years (Luterbacher *et al.* 2004). A comparison of the reconstructed historical temperature trend (mobile mean of 25 years) and the SV1 $\delta^{18}\text{O}_c$ profile (Fig. 6) shows that low temperature anomalies coincide with $\delta^{18}\text{O}_c$ minima. The trend toward increasing temperature anomalies since AD 1700 is also paralleled by the stalagmite $\delta^{18}\text{O}_c$ trend. There is thus a positive $d\delta^{18}\text{O}_c/dT$ relationship. By taking into account the resolution of the isotope samples (25 years toward the top of the stalagmite) and comparing a mobile mean of 25 years for the temperature anomaly reconstructed by Luterbacher *et al.* (2004) with the SV1 $\delta^{18}\text{O}_c$ series for the past 500 years, we found that a 1°C rise in mean

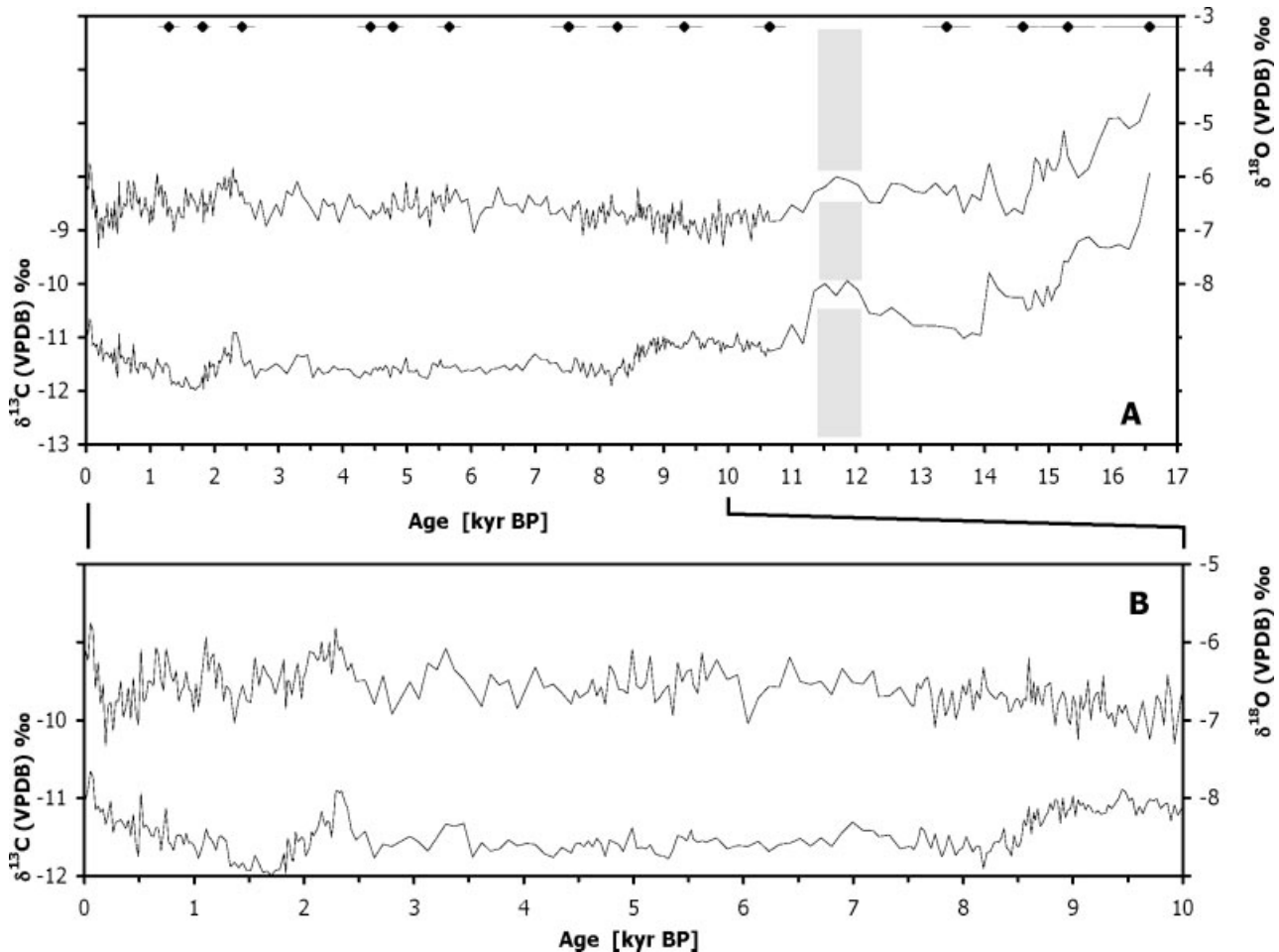


Fig. 5. A. Carbon and oxygen isotopic variability for the past c. 17 kyr measured along the growth axis of SV1 with the position of the U/Th ages shown with 2σ error bars (top). The grey area between 12.1 and 11.3 kyr BP corresponds to a honey-coloured layer in the stalagmite. The Holocene portion of the stable isotope profiles shows muted variability with respect to the Lateglacial. B. Enlargement showing the muted stable isotopes variability for the Holocene.

annual temperature (over 25 years) corresponds to a 2.85‰ increase of the SV1 $\delta^{18}\text{O}_c$ (over 25 years). Because the Holocene portion of the stalagmite has formed in quasi-isotopic equilibrium it is reasonable to assume that the present-day relationship between $\delta^{18}\text{O}_c$ and $\delta^{18}\text{O}_w$ remained similar throughout the Holocene. A shift toward higher $\delta^{18}\text{O}_c$ values therefore indicates warmer mean annual temperatures, as already observed in an Alpine speleothem from NE Italy (McDermott *et al.* 1999). By coupling the modern relationship between $\delta^{18}\text{O}_p$ and mean annual air temperature of 0.6‰/°C for mid-Europe (Rozanski *et al.* 1993) with the calcite/water fractionation, which, at the mean annual temperature of the cave is $-0.22\text{‰}/^\circ\text{C}$ (O'Neil *et al.* 1969), a net positive shift of $\delta^{18}\text{O}_c$ of c. 0.38‰/°C is obtained. This theoretical value is lower than that obtained through the calibration. The dampened sensitivity of SV1 $\delta^{18}\text{O}_c$ with respect to the theoretical $\delta^{18}\text{O}_c$ -temperature relationships depends on several factors. One is the resolution of the $\delta^{18}\text{O}_c$

data, which, for the past 500 years in SV1 is 25 years. An improved resolution would allow $\delta^{18}\text{O}_c$ peaks to be detected that are smoothed (see, for example, McDermott *et al.* 2001). We were, however, at the limit of the present state of our analytical technique. The second factor is the damping effect of the Mediterranean on rainfall oxygen isotope composition with respect to the Alpine and Central European values (Darling 2004). Proximity to the sea seems to have protected the karst area of Trieste from much temperature change.

Holocene temperature variability in the SE Alps

Although we are not fully confident of the accuracy of temperature estimates based on the present day calibration, which does not account for changes in storm tracks and 'amount effect', we reconstruct a slow temperature rise of c. 0.5°C since 10 kyr BP. The trend indicates close agreement with the temperature

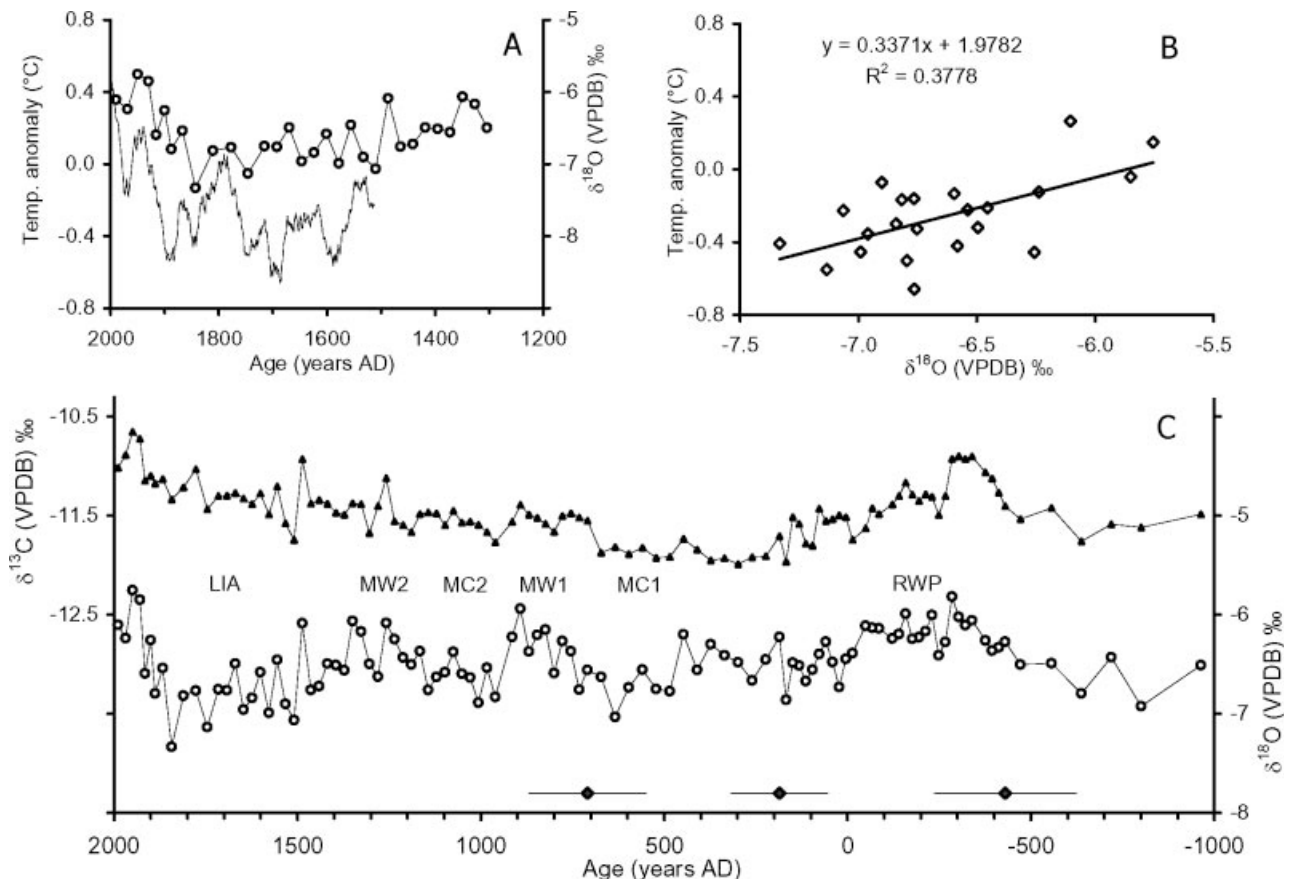


Fig. 6. Reconstruction of climate variability over the last 3 kyr from SV1 isotope record. A. Calibration of SV1 $\delta^{18}\text{O}_e$ (line with open circles) with the temperature anomaly reconstruction for the past 500 years (Luterbacher *et al.* 2004; running mean = 25 years; continuous line). B. Reconstructed relationship between SV1 $\delta^{18}\text{O}_e$ variations and the temperature anomaly from Luterbacher *et al.* (2004), whereby each 1°C temperature deviation from the present-day mean results in an enrichment of 2.85‰ in $\delta^{18}\text{O}_e$. C. C and O isotope records of SV1 for the last 3 kyr (time resolution = 25 years): LIA = Little Ice Age; MW1 and MW2 = Medieval Warm Periods; MC1 and MC2 = Medieval Cold Periods; RWP = Roman Warm Period. The positions of the corrected U/Th ages are plotted with 2σ error bars at the bottom. The RWP and MW1 and 2 were characterized by temperatures similar to those of the past 100 years (see text for details).

reconstruction for SE Europe from pollen data, but the inferred rise from SV1 is about 0.5°C lower. This discrepancy could be due to the damping effect on the local climate of the Adriatic Sea (about 20 km distant throughout the Holocene) with respect to most of the pollen archives for SE Europe that are intracontinental (Davis *et al.* 2003). The warmest temperatures in the Holocene were probably reached between *c.* 400 BC (2400 years ago) and *c.* 0 AD (Roman Warm Period, RWP in Fig. 6C). According to our reconstruction, in the RWP temperatures were similar to those of today or even slightly warmer. The $\delta^{18}\text{O}_e$ values of the RWP in a stalagmite from SW Ireland are also similar to those of the past 100 years (McDermott *et al.* 2001; McDermott 2004). The SV1 record shows a complex structure for the medieval climate. The first cool phase occurred from *c.* AD 450 to *c.* AD 700 (MC1 in Fig. 6C), and was followed by the first warming from *c.* AD 700 to *c.* AD 850 (coinciding with the Carolingian Empire) (MW1 in Fig. 6C). The second

Medieval Cold Period (MC2 in Fig. 6C) was recorded by SV1 from *c.* AD 900 to AD 1100. SV1 $\delta^{18}\text{O}$ record identifies a cold spell at about the year AD 1000, for which global mean surface temperature reconstructions based on high-resolution proxy temperature records indicate a temperature anomaly of -0.2°C with respect to the 1961–1990 instrumental reference period (Mann & Jones 2003). The second warming occurred from *c.* AD 1150 to *c.* AD 1400, for which temperatures seem to have been similar to those of today (MW2 in Fig. 6C). A similar complex temperature structure is also recorded by the Irish stalagmite (McDermott *et al.* 2001; McDermott 2004). Regional speleothem data thus indicate that the single ‘Medieval’ interval of moderately warm conditions from about AD 800 to 1400, as reconstructed by Mann & Jones (2003), was actually characterized by climate instability (at least in the Northern Hemisphere).

SV1 records the coldest period of the past 2000 years from AD 1450 to 1800, which coincides with the

Little Ice Age (LIA). In the period AD 1650 to 1750, which broadly coincides with the Maunder Minimum (MM; 1645–1715) coldest phase of the LIA in Europe and in the Alps (Wanner *et al.* 2000; Luterbacher *et al.* 2004), the estimated temperature anomaly with respect to the present is *c.* -1°C for the extremes. Because of the resolution (25 years) and the damping effect of the Mediterranean, SV1 does not record the extreme temperature anomaly of -3.7°C reconstructed by Luterbacher (2001) for the coldest years of the MM in Central Europe. In SV1, the decade centred at AD 1840 is the last coldest phase of the LIA. In the past 100 years, temperature rose sharply (Fig. 6A) and followed the Northern Hemisphere temperature trend reconstructed by Mann *et al.* (1999), which is also recorded by a stalagmite from Alps of NE Italy (Frisia *et al.* 2003).

SV1 shows Holocene mean $\delta^{13}\text{C}_c$ values of $-11.44 \pm 0.22\text{‰}$, which are typical of continental carbonates and speleothems deposited in equilibrium with the C3 vegetation of temperate regions (Cerling *et al.* 1991; Baker *et al.* 1997).

Stalagmite growth rate in temperate settings is controlled by temperature, the amount of CO_2 available in the soil and drip rate (Kaufmann 2003; Kaufmann & Dreybrodt 2004). Drip rate can limit growth at slow dripping sites. In our experience, however, we observed that changes in drip rates in Alpine stalagmites commonly resulted in fabric changes (Frisia *et al.* 2000). In particular, columnar fabric, which is typical of constant drip rate, is replaced by microcrystalline or dendritic fabric if drips show strong seasonal variability. SV1 consists of the same elongated columnar fabric. We, therefore, assume that drip rate variability was not a limiting factor.

In recent Alpine stalagmites, temperature controls growth rate via the duration of winter frozen soil conditions (Frisia *et al.* 2003). SV1 records its highest extension rate in the time period *c.* 10.6 to *c.* 7.5 kyr BP, when the $\delta^{18}\text{O}_c$ values were lighter than today and, if the $\delta^{18}\text{O}_c$ –temperature relationship observed for the past 500 years still held, mean annual temperatures could have been lower than at the present day, but winter temperatures may have been relatively mild. The Early Holocene winter temperatures reconstruction for SW Europe based on pollen data indicates temperature anomalies up to *c.* $+2^{\circ}\text{C}$ with respect to present-day (Davis *et al.* 2003). Bar-Matthews *et al.* (2003) showed that in the Early Holocene the annual rainfall in the Eastern Mediterranean was higher than today, and therefore we do not exclude influence of the amount effect on both $\delta^{18}\text{O}_c$ and growth rate from *c.* 10.6 to *c.* 7.5 kyr BP. In SV1, growth rate slowed to *c.* $11 \mu\text{m}/\text{yr}$ after 4.4 kyr BP, when Holocene temperature reconstruction based on the $\delta^{18}\text{O}_c$ temperature calibration indicates warmer conditions. Early Holocene extension rates were high in stalagmites from the NE Italian Alps, SW Ireland and Sauerland

(McDermott *et al.* 1999; Niggemann *et al.* 2003) in a period for which pollen data indicate cooler temperatures than after 6 kyr BP (Guiot *et al.* 1993; Davis *et al.* 2003). It is, therefore, possible that the extension rate–temperature relationship did not hold for the Early Holocene, when the Mediterranean region was characterized by wetter conditions (Bar-Matthews *et al.* 2003). Orbital variations may be a fundamental cause of this phenomenon. Higher summer insolation in the Alps may have resulted in enhanced rainfall and stronger seasonal contrast than today (Crucifix *et al.* 2002; Bradley *et al.* 2003), which shifted the stalagmite growth season. Extension rate in the Early Holocene might have been controlled by summer temperatures and rainfall.

Lateglacial climate in the SE Alps

The calibration with the present may not hold true for the Lateglacial, when climate was still in a ‘glacial mode’ (Kolodny *et al.* 2003), the cave was located 500 to 300 km north of the coastline (Lambeck *et al.* 2004) in a more continental setting, and speleothem deposition may not have occurred in isotopic equilibrium (Fig. 2). SV1 extension rate was very slow up to *c.* 10.6 kyr. The drop in $\delta^{18}\text{O}_c$ since 16.5 kyr BP correlates with the sharp drop observed in speleothems from Soreq cave (Israel) starting at *c.* 17 kyr BP (Bar-Matthews *et al.* 2003), which were attributed to a temperature increase and ice-sheet melting during the last deglaciation (Bar-Matthews *et al.* 1999). The structure of the last deglaciation differs from that in Greenland, however, where it is characterized by two major abrupt warming spells at 14.6 (Bølling) and 11.6 kyr BP (Blunier *et al.* 1998), and Antarctica, where temperature increased from at least 18.5 kyr BP (Blunier *et al.* 1998). The last interglacial palaeoclimate changes in the SE margin of the Alps appear compatible with both the early ending of full glacial conditions in Antarctica and the steps toward full interglacial climates recorded in Greenland. By contrast, a composite speleothem record from NW Germany spanning the last 17.6 kyr shows connections with Greenland, i.e. no deposition during the cold phases GS-2 and GS-1 (YD) and a very short depositional stage in GI-1a (Bølling–Allerød) (Niggemann *et al.* 2003).

The extension rates and $\delta^{18}\text{O}_c$ record for the late deglaciation in SV1 are interpreted here as a combination of temperature and rainfall, with rainfall exerting the dominant effect (Bar-Matthews *et al.* 1997, 1999). According to the model proposed by Bar-Matthews *et al.* (1997), the $\delta^{18}\text{O}_c$ depletion at *c.* 14.5 kyr BP is interpreted as reflecting warm and wet conditions. The GS-1 (YD) is characterized by a shift toward higher $\delta^{18}\text{O}_c$ values, coinciding with $\delta^{13}\text{C}_c$ enrichment of up to $+1\text{‰}$ (Fig. 7) from 12.0 and 11.4 kyr BP, while the extension rate is extremely

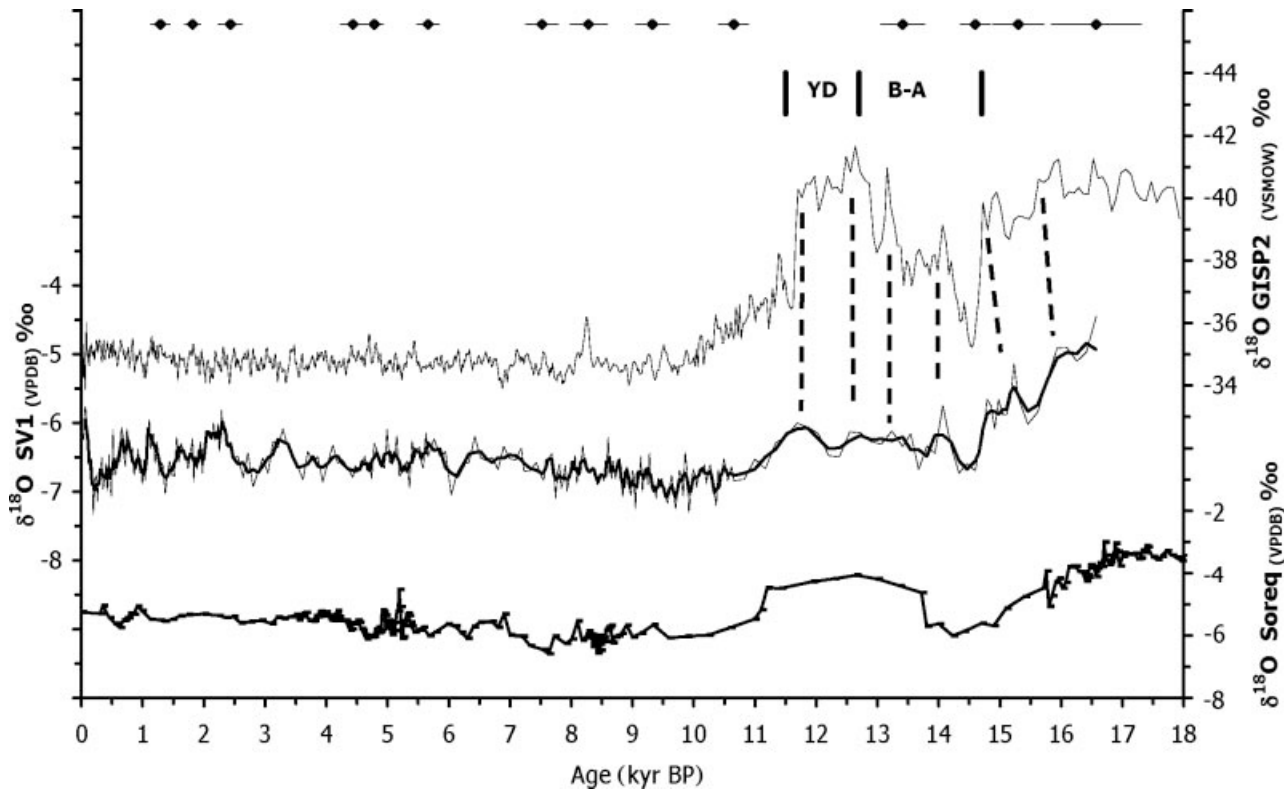


Fig. 7. Comparison between the SV1 oxygen isotope record, the Greenland GISP2 ice core $\delta^{18}\text{O}$ (note inverted scale – Grootes *et al.* 1993) and the $\delta^{18}\text{O}_c$ speleothem record from Soreq Cave in Israel (Bar-Matthews *et al.* 2003). The position of the U/Th ages of SV1 are plotted with 2σ error bars at the top. YD = Younger Dryas; B–A = Bølling–Allerød interstadial. (Last Glacial and Interglacial Greenland event-stratigraphy from Lowe *et al.* 2001).

low ($<8 \mu\text{m}/\text{yr}$). These characteristics indicate that the YD was most probably characterized by cool and arid conditions, which is consistent with pollen data (Guiot *et al.* 1993). Lake level records in the Jura mountains provide evidence for climatic drying during the late GS-1 and the GS-1 to Preboreal transition (Magny *et al.* 2003). By contrast, the relatively high lake levels in the YD at Gerzensee (Switzerland) were interpreted as due to reduced percolation of water into the shallow groundwater as a result of frozen soil conditions, which increased direct runoff in the lake (von Grafenstein *et al.* 2000). Similarly, reduced percolation due to prolonged frozen soil conditions, associated with decreased precipitation may have diminished the recharge of the karst aquifer in the Savi cave area during the YD. The $\delta^{13}\text{C}_c$ peak for the YD, which is better defined than the $\delta^{18}\text{O}_c$, can be interpreted as reflecting cold and arid climate, which yielded a short duration of active soil condition and the related decrease of soil CO_2 production (cf. Frisia *et al.* 2003; Genty *et al.* 2003). The $\delta^{18}\text{O}_c$ peak recorded by SV1 in the YD broadly coincides with a similar $\delta^{18}\text{O}_c$ peak at Soreq Cave (Bar-Matthews *et al.* 2003), supporting a connection between the SE margin of the Alps and the Eastern Mediterranean. Bar-Matthews *et al.* (2003) calculated high $\delta^{18}\text{O}$ values of rainwater for the YD, at

c. 5 kyr and for the last 3.5 kyr. They did not provide palaeo-annual rainfall calculations for the YD, but associated the high $\delta^{18}\text{O}$ at *c.* 5.1 kyr with an abrupt drop in average rainfall amount and, similarly, estimated low average rainfall amounts for the past 3 kyr. The high $\delta^{18}\text{O}_c$ values recorded in the YD may, therefore, reflect a combination of low rainfall amount and high rainfall $\delta^{18}\text{O}$. A comparison with the $\delta^{18}\text{O}$ record of GISP2 ice core (Grootes *et al.* 1993) shows that shifts to depleted oxygen in Greenland (cold) correspond to high $\delta^{18}\text{O}_c$ values in the SV1 and Soreq $\delta^{18}\text{O}_c$ profiles (dry) (Fig. 7). Bar-Matthews *et al.* (1999) hypothesized that the higher $\delta^{18}\text{O}$ values of the Lateglacial portion of the Soreq cave record indicate a major change in the way the Mediterranean Sea affected rainfall. Similarly, in SV1 the $\delta^{18}\text{O}_c$ values are higher in the Lateglacial and may reflect a close connection between the SE margin of the Alps and the Mediterranean region.

The isotope record of SV1 indicates that the Lateglacial climate in the SE Alpine region was dominated by shifts from arid to humid periods. The marked glacial climate instability observed in the SV1 speleothem supports the hypothesis that Late Palaeolithic Alpine art was a consequence of these harsh conditions, which required a deep knowledge of the

environment to be transmitted by paintings as proposed by Mithen (2003). After the YD there was no need for such knowledge any more.

Conclusions

SV1 provides the first continuous European climate proxy record from a stalagmite for the past *c.* 17 kyr BP, and the first evidence for the different effects of the glacial and the Holocene climate modes in the SE Alpine region. During the Lateglacial, the oxygen isotope variability is in broad agreement with the speleothem record from the Eastern Mediterranean, and is interpreted as being dominated by greater instability of the rainfall record under glacial boundary conditions. The YD is characterized by low extension rate, high C and O isotopes indicating cold and arid conditions for the SE margin of the Alps. In the Holocene there is a positive relationship between temperature and $\delta^{18}\text{O}_c$. We identified a slow, steady temperature rise of *c.* 0.5°C from 10 kyr BP to the present. This trend is in broad agreement with the area-average mean annual temperature anomalies reconstructed for the SE European region from pollen data. The high-resolution record for the past 3 kyr identifies the Roman Warm Periods and two Medieval Warm Periods characterized by temperatures that were similar to the present. The LIA stands out as one of the coldest periods of the Holocene, with estimated mean annual temperatures of *c.* 1°C cooler relative to today.

Acknowledgements. – We are very grateful to P. Tuccimei for performing six U/Th analyses, R. Miorandi for micromilling and drilling, M. Wimmer for assistance with the stable isotope analyses, P. Forti, M. Potleca, L. Zini and U. Sauro for logistics. We thank M. Bar-Matthews for providing the updated Soreq record and for critical revision of the manuscript. The research was funded by MIUR-COFIN 2000 project and by the Provincia Autonoma di Trento (University and Scientific Research Service, project AQUAPAST).

References

- Baker, A., Ito, E., Smart, P. L. & McEwan, R. F. 1997: Elevated and variable $\delta^{13}\text{C}$ in speleothems in a British cave system. *Chemical Geology* 136, 263–270.
- Bar-Matthews, M., Ayalon, A. & Kaufman, A. 1997: Late Quaternary paleoclimate in the Eastern Mediterranean Region from stable isotope analysis of speleothems in Soreq Cave Israel. *Quaternary Research* 47, 155–168.
- Bar-Matthews, M., Ayalon, A., Kaufman, A. & Wasserburg, G. J. 1999: The eastern Mediterranean paleoclimate as a reflection of regional events: Soreq cave, Israel. *Earth and Planetary Science Letters* 166, 85–95.
- Bar-Matthews, M., Ayalon, A., Gilmour, M., Matthews, A. & Hawkesworth, C. 2003: Sea–land oxygen isotopic relationships from planktonic foraminifera and speleothems in the Eastern Mediterranean region and their implication for palaeorainfall during interglacial intervals. *Geochimica et Cosmochimica Acta* 67, 3181–3199.
- Beniston, M. & Junco, P. 2002: Shifts in the distribution of pressure, temperature and moisture and changes in the typical weather patterns in the Alpine region in response to the behaviour of the North Atlantic Oscillation. *Theoretical and Applied Climatology* 71, 29–42.
- Blunier, T., Chappellaz, J., Schwander, J., Dallenbach, A., Stauffer, B., Stocker, T., Raynaud, D., Jouzel, J., Clausen, H. B., Hammer, C. U. & Johnsen, S. J. 1998: Asynchrony of Antarctic and Greenland climate change during the last glacial period. *Nature* 394, 39–743.
- Bradley, R. S., Briffa, K. R., Cole, J., Huges, M. K. & Osborn, T. J. 2003: The climate of the last millennium. In Alverson, K. D., Bradley, R. S. & Pedersen, T. F. (eds.): *Paleoclimate, Global Change and the Future*, 105–141. Springer, Berlin and Heidelberg.
- Cerling, T. E., Quade, J., Solomon, D. K. & Bowman, J. R. 1991: On the carbon isotopic composition of soil carbon dioxide. *Geochimica et Cosmochimica Acta* 55, 3403–3405.
- Cheng, H., Edwards, R. L., Hoff, J., Gallup, C. D., Richards, D. A. & Asmeron, Y. 2000: The half-lives of uranium-234 and thorium-230. *Chemical Geology* 169, 17–33.
- Craig, H. 1961: Isotopic variations in meteoric waters. *Science* 133, 1702–1703.
- Crucifix, M., Loutre, M.-F., Tulkens, P., Fichefet, T. & Berger, A. 2002: Climate evolution during the Holocene: a study with an Earth system model of intermediate complexity. *Climate Dynamics* 19, 43–60.
- Dalmeri, G., Cusinato, A., Bassetti, M., Kompatscher, K. & Hrozny-Kompatscher, M. 2004: The Epigravettian Mobiliary art of the Dalmeri rock-shelter (Trento, Northern Italy). *International Newsletter on Rock Art* 40, 15–24.
- Darling, W. G. 2004: Hydrological factors in the interpretation of stable isotopic proxy data present and past: a European perspective. *Quaternary Science Review* 23, 743–770.
- Davis, B. A. S., Brewer, S., Stevenson, A. C., Guiot, J. & Data contributors 2003: The temperature of Europe during the Holocene reconstructed from pollen data. *Quaternary Science Reviews* 22, 1701–1716.
- Frisia, S., Borsato, A., Fairchild, I. J. & McDermott, F. 2000: Calcite fabrics, growth mechanisms, and environments of formation in speleothems from the Italian Alps and Southwestern Ireland. *Journal of Sedimentary Research* 70, 1183–1196.
- Frisia, S., Borsato, A., Preto, N. & McDermott, F. 2003: Late Holocene annual growth in three Alpine stalagmites records the influence of solar activity and the North Atlantic Oscillation on winter climate. *Earth and Planetary Science Letters* 216, 411–424.
- Genty, D., Blamart, D., Ouahdi, R., Gilmour, M., Baker, A., Jouzel, J. & Van-Exeter, S. 2003: Precise dating of Dansgaard–Oeschger climate oscillations in western Europe from stalagmite data. *Nature* 421, 833–837.
- von Grafenstein, U., Eicher, U., Erlenkeuser, H., Ruch, P., Schwander, J. & Amman, B. 2000: Isotope signature of the Younger Dryas and two minor oscillations at Gerzensee (Switzerland): palaeoclimatic and palaeolimnologic interpretation based on bulk and biogenic carbonates. *Palaeogeography, Palaeoclimatology, Palaeoecology* 159, 215–229.
- Grotes, P. M., Stuiver, M., White, J. W. C., Johnsen, S. & Jouzel, J. J. 1993: Comparison of oxygen isotope records from the GISP2 and GRIP Greenland ice cores. *Nature* 366, 552–554.
- Guiot, J., de Beaulieu, J. L., Cheddadi, R., David, F., Ponel, P. & Reille, M. 1993: Climate in Western Europe during the last Glacial/Interglacial cycle derived from pollen and insect remains. *Palaeoceanography, Palaeoclimatology, Palaeoecology* 103, 73–93.
- Hendy, C. H. 1971: The isotopic composition of speleothems. – I. The calculations of the effects of different modes of formation on the isotopic composition of speleothems and their applicability as

- paleoclimatic indicators. *Geochimica Cosmochimica Acta* 35, 801–824.
- Kaufmann, G. 2003: Stalagmite growth and palaeo-climate: a numerical perspective. *Earth and Planetary Science Letters* 214, 251–266.
- Kaufmann, G. & Dreybrodt, W. 2004: Stalagmite growth and palaeoclimate: an inverse approach. *Earth and Planetary Science Letters* 224, 529–545.
- Kolodny, Y., Bar-Matthews, M., Ayalon, A. & McKeegan, K. D. 2003: A high spatial resolution $\delta^{18}\text{O}$ profile of a speleothem using an ion microprobe. *Chemical Geology* 97, 21–28.
- Lambeck, K., Antonioli, F., Purcell, A. & Silenzi, S. 2004: Sea level change along the Italian coast for the past 10,000 yrs. *Quaternary Science Reviews* 23, 1567–1598.
- Lauritzen, S. E. & Lundberg, J. 1999: Calibration of the speleothem delta function: an absolute temperature record for the Holocene in northern Norway. *The Holocene* 9, 659–669.
- Longinelli, A. & Selmo, E. 2003: Isotopic composition of precipitation in Italy: a first overall map. *Journal of Hydrology* 270, 75–88.
- Lowe, J. J., Hoek, W. Z. & INTIMATE group 2001: Inter-regional correlation of paleoclimatic records for the Last Glacial–Interglacial Transition: a protocol for improved precision recommended by the INTIMATE group. *Quaternary Science Reviews* 20, 1175–1187.
- Ludwig, K. R. 1999: Using Isoplot/Ex, Version 2.01: A geochronological toolkit for Microsoft Excel. *Berkeley Geochronology Center Special Publication 1a*, 1–55.
- Ludwig, K. R. 2003: Mathematical–statistical treatment of data and errors for $^{230}\text{Th}/\text{U}$ geochronology. *Reviews Mineralogy Geochemistry* 52, 631–636.
- Luterbacher, J. 2001: The Late Maunder Minimum (1675–1715). Climax of the Little Ice Age in Europe. In Jones, P., Ogilvie, A. E. J., Davies, T. D. & Briffa, K. R. (eds.): *History and Climate Memories of the Future?* 29–54. Kluwer Academic/Plenum Publishers, New York.
- Luterbacher, J., Dietrich, D., Xoplaki, E., Grosjean, M. & Wanner, H. 2004: European seasonal and annual temperature variability, trends, and extremes since 1500. *Science* 303, 1499–1503.
- Magny, M., Thew, N. & Hadorn, P. 2003: Late-glacial and early Holocene changes in vegetation and lake-level at Hauterive/Rouges Terres, Lake Neuchatel (Switzerland). *Journal of Quaternary Science* 18, 31–40.
- Mann, M. E., Bradley, R. S. & Huges, M. K. 1999: Northern Hemisphere temperatures during the past millennium: inferences, uncertainties and limitations. *Geophysical Research Letters* 26, 759–762.
- Mann, M. E. & Jones, P. D. 2003: Global surface temperature over the past two millennia. *Geophysical Research Letters* 30, 1820–1824.
- McDermott, F. 2004: Palaeo-climate reconstruction from stable isotope variations in speleothems: a review. *Quaternary Science Reviews* 23, 901–918.
- McDermott, F., Frisia, S., Yiming, H., Longinelli, A., Spiro, B., Heaton, T. H. E., Hawkesworth, C. J., Borsato, A., Keppens, E., Fairchild, I. J., van der Borg, K., Verheyden, S. & Selmo, E. 1999: Holocene climate variability in Europe: evidence from $\delta^{18}\text{O}$, textural and extension-rate variations in three speleothems. *Quaternary Science Reviews* 18, 1021–1038.
- McDermott, F., Matthey, D. P. & Hawkesworth, C. J. 2001: Centennial-scale Holocene climate variability revealed by a high-resolution speleothem $\delta^{18}\text{O}$ record from SW Ireland. *Science* 294, 1328–1331.
- Mithen, S. 2003: *After the Ice*. 622 pp. Phoenix, London.
- Niggemann, S., Mangini, A., Richter, D. K. & Wurth, G. 2003: A palaeoclimate record of the last 17,600 years in stalagmites from the B7 cave, Sauerland, Germany. *Quaternary Science Reviews* 22, 555–567.
- O’Neil, J. R., Clayton, R. N. & Mayeda, T. K. 1969: Oxygen isotope fractionation in divalent metal carbonates. *Journal of Chemical Physics* 51, 5547–5558.
- Rozanski, K., Araguás-Araguás, L. & Gonfiantini, R. 1993: Isotopic patterns in modern precipitation. In Swart, P. K., Lohmann, K. C., McKenzie, J. A. & Savin, S. (eds.): *Climate Change in Continental Isotopic Records*, 1–36. Geophysical Monograph 78. American Geophysical Union, Washington DC.
- Wanner, H., Holzhauser, H. P., Pfister, C. & Zumbühl, H. 2000: Interannual to century scale climate variability in the European Alps. *Erdkunde (Earth Science)* 54, 167–175.

Appendix

For the present study, we applied a novel strategy for U/Th dating when stalagmites show detrital contamination. In SV1, detrital Th contamination characterized all the samples, even though high Th contamination was detected in only two specimens at the bottom of the stalagmite. We used the ISOPLOT code Th-correction function (Ludwig 1999) on three pairs of quasi co-genetic specimens (SV1-24/-25; SV1-238/-27; and SV1-249/-28) to calculate the $^{230}\text{Th}/^{232}\text{Th}$ activity ratio of the detrital component that minimizes the age discrepancy of the two cogenetic samples within each pair by successive iterations. The pairs SV1-24/-25 and SV1-238/-27 have a high and similar $^{230}\text{Th}/^{232}\text{Th}$ activity ratio. By contrast, the pair SV1-249/-28 is characterized by very different $^{230}\text{Th}/^{232}\text{Th}$ activity ratios (11.8 and 103.3, respectively), and

therefore the sensitivity of the correction is mostly tuned by the discrepancy of this pair. The calculated $^{230}\text{Th}/^{232}\text{Th}$ activity ratio of the detrital component that eliminates the age discrepancy for the SV1-249/-28 pair is $1.34^{+0.31}/_{-0.25}$ (95% confidence limits). The calculation accounts for the fact that SV1-249 was taken 1 mm above SV1-28: this distance corresponds to 60 years at the estimated growth rate of $17\ \mu\text{m}/\text{year}$. The calculated ages, which corresponded to the 95% confidence limits of +0.31 and –0.25, were utilized to propagate the errors in the corrected ages. The $^{230}\text{Th}/^{232}\text{Th}$ activity ratio of $1.34^{+0.31}/_{-0.25}$ optimizes the age agreement for the SV1-24/-25 and SV1-238/-27 pairs, and eliminates the age inversion for the SV1-207. This value falls within the range of the mean bulk Earth value of 0.8 ± 0.8 (see Ludwig 2003).